

An Aurone Derivative Revealing the Metabolism of Lipid Droplets and Monitoring Oxidative Stress in Living Cells

Kang-Nan Wang, Shuyue Ma, Yanyan Ma, Yuping Zhao,
Miaomiao Xing, Liyu Zhou, Duxia Cao, and Weiyong Lin

Anal. Chem., **Just Accepted Manuscript** • DOI: 10.1021/acs.analchem.0c00456 • Publication Date (Web): 10 Apr 2020

Downloaded from pubs.acs.org on April 10, 2020

Just Accepted

“Just Accepted” manuscripts have been peer-reviewed and accepted for publication. They are posted online prior to technical editing, formatting for publication and author proofing. The American Chemical Society provides “Just Accepted” as a service to the research community to expedite the dissemination of scientific material as soon as possible after acceptance. “Just Accepted” manuscripts appear in full in PDF format accompanied by an HTML abstract. “Just Accepted” manuscripts have been fully peer reviewed, but should not be considered the official version of record. They are citable by the Digital Object Identifier (DOI®). “Just Accepted” is an optional service offered to authors. Therefore, the “Just Accepted” Web site may not include all articles that will be published in the journal. After a manuscript is technically edited and formatted, it will be removed from the “Just Accepted” Web site and published as an ASAP article. Note that technical editing may introduce minor changes to the manuscript text and/or graphics which could affect content, and all legal disclaimers and ethical guidelines that apply to the journal pertain. ACS cannot be held responsible for errors or consequences arising from the use of information contained in these “Just Accepted” manuscripts.

An Aurone Derivative Revealing the Metabolism of Lipid Droplets and Monitoring Oxidative Stress in Living Cells

Kangnan Wang,^{†, ‡} Shuyue Ma,[†] Yanyan Ma,[†] Yuping Zhao,[†] Miaomiao Xing,[†] Liyu Zhou,[‡] Duxia Cao,^{*, †} Weiyin Lin,^{*, †}

[†] School of Materials Science and Engineering, Institute of Fluorescent Probes for Biological Imaging, University of Jinan, Jinan, 250022, Shandong, China *E-mail: duxiacao@ujn.edu.cn; weiyinlin2013@163.com.

[‡] Shunde Hospital, Southern Medical University (The First People's Hospital of Shunde), Foshan, 528308, Guangdong, China

ABSTRACT: Lipid droplets (LDs) are closely connected with many physiological processes and abnormal LDs are related to many diseases. Herein, a family of two-photon fluorescence compounds based on the aurone skeleton were developed as efficient LDs imaging probes. They exhibit the obvious solvatochromism effect from blue to orange emission (~140 nm shift) in various solvents. The robust probes possess low toxicity to living cells, high photobleaching resistance and superior photostability and can light up LDs with high specificity. Furthermore, the probe **DMMB** was carefully applied in real-time monitoring the morphological changes of LDs and the interactions between LDs and mitochondria under specific physiological conditions (e.g. starvation). We have observed for the first time the dynamic change between mitochondria and LDs when mitochondrial damage is caused by a large excess of H₂O₂ in a short time.

Lipid droplets (LDs), mainly enriching various neutral lipids including cholesteryl ester and triacylglycerol, are recognized as inert reservoirs for energy storage and reports on the fine function of LDs are rarely declared for a long time.¹⁻⁴ Inspiringly, recent evidences indicate that LDs are closely connected with lots of physiological processes and related to the metabolism of lipids, signal transduction and even cell apoptosis.^{5,6} LDs are neutral lipid storage organelles, which provide accessible and fast fatty acids (FAs) sources for energy during nutritional deprivation. Miraculously, during long-term starvation, lipids released by autophagy/apoptosis of membrane organelles are packaged and stored in new LDs.⁵ Additionally, it should be highlighted that the abnormal accumulation of LDs is related to many diseases involving obesity, hyperlipidemia, hepatocellular carcinoma, inflammation, atherosclerosis and cancer.⁷⁻⁹ Therefore, it is of significance to monitor LDs accurately for the exploration of their biological metabolism contributing to the early diagnosis of related diseases.

Subcellular organelles (such as mitochondria, LDs, etc.) produce a variety of stress responses when living cells are stimulated by the external environment.^{10,11} For example, intracellular excess reactive oxygen species (ROS) can cause changes in mitochondrial membrane potential (MMP) and even induce apoptosis.^{12,13} When cells are in deprivation from nutrition (starvation), they will activate related mechanisms (such as autophagy) to synthesize a large amount of energy substances storing in LDs to meet the needs of future survival.^{14,15} In this process, there are also polarity changes in many organelles (such as mitochondria, LDs, etc.).^{16,17} Recently, Tang's group reported a LDs-specific dye **TPAP-BB**, which was used to track the dynamic autophagy process between LDs and mitochondria in the case of ROS inducing apoptosis.¹⁸ Anila et al. reported a fluorescent dye **DXB-NIR** used to monitor the changes in LDs polarity derived from fundamental nutrition and oxidative stress.¹⁹ According to the reports from the literatures,^{20,21} large excess of H₂O₂ can directly stimulate cells to produce oxidative stress

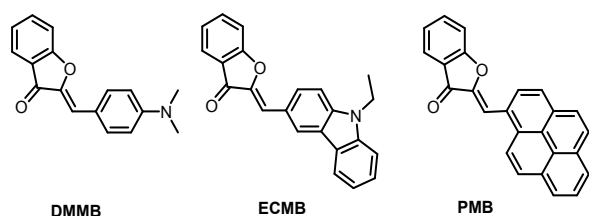


Figure 1. Molecular structures of the probes.

response in a short time and result in MMP collapse or even damage. However, it is not clear what happens between mitochondria and LDs when mitochondrial damage is caused by a large excess of ROS in a short time.

It is significant to track LDs accurately for exploring their biological metabolism devoting to the early diagnosis of related diseases. However, the common experimental methods require cell fixation. Moreover, proteins associated with LDs are seldomly monitored after the permeabilization.²² A widely used method is visualizing FAs trafficking with a fluorescent FAs probe.^{23,24} Fluorescent labeling of FAs is a complex process and may be at risk of miss targeting and photobleaching. On the other hand, despite being the commercially available probes to staining LDs, BODIPY 493/503, Nile Red and Oil Red O face many limitations such as specificity, photostability, small Stokes shifts, and large background noise, etc.² Thus, fluorescent small dyes with excellent photophysical properties, staining the lipid core of native LDs, and being able to be used to monitor LD-related biological events are urgently needed.

Hence, we described three efficient LDs markers based on aurone skeleton with dimethylamino (**DMMB**), N-ethylcarbazolyl (**ECMB**) and pyrene (**PMB**) as the terminal groups (Figure 1), which have been described as the two-photon fluorescence materials by our group.²⁵ Strikingly, **DMMB** presents a dotted shape distribution in the cells and demonstrates the accumulation around LDs. Co-stain experiments of these probes with BODIPY493/503 reveal that **DMMB** can monitor LDs with high Pearson's correlation efficiency up to 0.983. The applications of **DMMB** for monitoring LDs in living cells have been investigated, which include inspecting the formation of LDs under oleic acid and transportation for free fatty acids from LDs to mitochondria in the process of autophagy under the condition of Hank's

balanced salt solution (HBSS) without serum. More importantly, we have observed for the first time the dynamic changes between mitochondria and LDs when mitochondrial damage is caused by a large excess of H₂O₂ in a short time.

MATERIALS AND METHODS

Cell culture and colocalization assay. A549 and HeLa cells were cultured as reported method.²⁶ A549 cells were first incubated with 10 μM of **DMMB/ECMB/PMB** for 30 min, and then further treated with BODIPY493/503 (1 μg/mL) for another 30 min. After that, the cells were washed by using phosphate buffered saline (PBS), and then viewed immediately on a confocal microscope (Carl Zeiss LSM 710).

Fluorescence microscopy imaging. A549 cells were reared into confocal plates and cultured for 24 h. Afterwards, the cells were cultivated with the probes for 30 min. All the cells were rinsed three times with PBS buffer solution ahead of confocal images.

Detection of oleic acid-induced accumulation of LDs. A549 cells were pre-treated with different concentrations (0, 100 μM, 200 μM) of oleic acid for 8 h. After that, cell media was replaced by fresh RPMI 1640 media containing 20 μM of **DMMB**. After staining for 30 min, cells were immediately subjected to cell imaging by confocal microscope.

Monitoring the dynamics of LDs during starvation. The starved A549 cells were incubated in HBSS for 8 h. And then, the starved and control cells were stained with **DMMB** (20 μM) and Mito Tracker Red (MTR, 100 nM) in HBSS and complete 1640 media, respectively, for 30 min. After that, the cells were observed with a confocal microscope.

Monitoring of the dynamics of LDs during oxidative stress.

After A549 cells were cultured in 35 mm dishes for 24h, the cells were incubated with **DMMB** (10 μ M) and Mito Tracker Deep Red (MTDR, 100 nM) for 30 min. And then, the cells were washed by using PBS and further incubated with H₂O₂ (10 mM) at for 20 min to induce oxidative stress. The treated cells were immediately observed under a confocal microscope for **DMMB** (λ_{ex} = 405 nm) and MTDR (λ_{ex} = 633 nm). In the comparative experiments, only MTDR was incubated in A549 cells for 30 min and washed with PBS. After that, A549 cells were immediately observed under the same conditions.

RESULTS AND DISCUSSION

Synthesis and spectral properties of the probes. These three aurone derivatives were synthesized through the cyclization reaction of corresponding hydroxychalcones under the catalyzation of mercuric acetate (Scheme S1), which have been reported as two-photon fluorescence materials by our group.²⁵ The selection of aurone molecular backbone is based on its large conjugation, potential strong fluorescence properties and low physiological toxicity.

UV-vis absorption and fluorescence spectra of the probes in different organic solvents (Figures 2, S1, S2 and Table S1) indicate that these probes show obvious fluorescence peaks red shift upon the increase of solvent polarity. Especially **DMMB** exhibits maximum fluorescence emission red shift from 450 nm, 480 nm (non-polar hexane) to 592 nm (polar DMSO) (Figure 2a). These probes are weakly emissive in pure water, while the fluorescence intensity grows gradually with increasing 1,4-dioxane volume content, accompanied with apparent blue-shifted maximum emission from 588 nm (**DMMB**, water) to 521 nm (**DMMB**, 1,4-dioxane) (Figure 2b) due to the intramolecular charge transfer effect. Particularly, **DMMB** exhibits stronger positive solvatochromism compared with **ECMB** and **PMB**. The lipophilicity determined by a classical shake-flask method²⁷ for the probes are distributed within 1.4-1.8. The high lipophilicity and high fluorescence emission in low polar solvents of the probes provide opportunities for their application in LDs imaging. Density functional theory (DFT, Figure S3) calculation exhibits that **DMMB** has higher dipole moment (6.24 Debye) relative to other two compounds (**ECMB**, 5.51 Debye, **PMB**, 2.91 Debye).

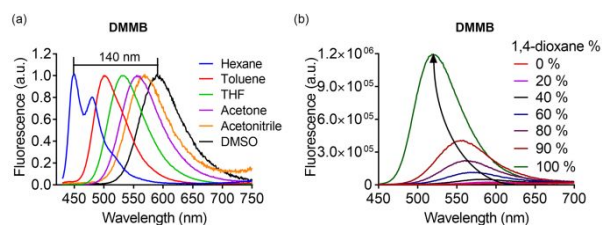


Figure 2. (a) Normalized fluorescence spectra of **DMMB** (10 μ M) in organic solvents of varying polarity. Fluorescence spectra of **DMMB** in the mixture of water and 1,4-dioxane with different proportions. (λ_{ex} = 405 nm).

To monitor LDs in cells under physiological environment, the probe should sustain stable at a wide pH range. Thus, the fluorescence spectra of the probes in various pH environments were separately measured. As shown in Figure S4(a), these probes are stable over a wide pH range (5.0-11.0), indicating the great potential in detecting LDs for biological applications in cells. Furthermore, an effective fluorescent probe should possess good selectivity in a complex biological system. The effect of various analytes on the fluorescence properties of **DMMB** was also detected. As shown in Figure S4(b), upon the excitation at 405 nm, other species have little interference with the fluorescence of **DMMB** at 550 nm, indicating that the probe is inert to these analytes.

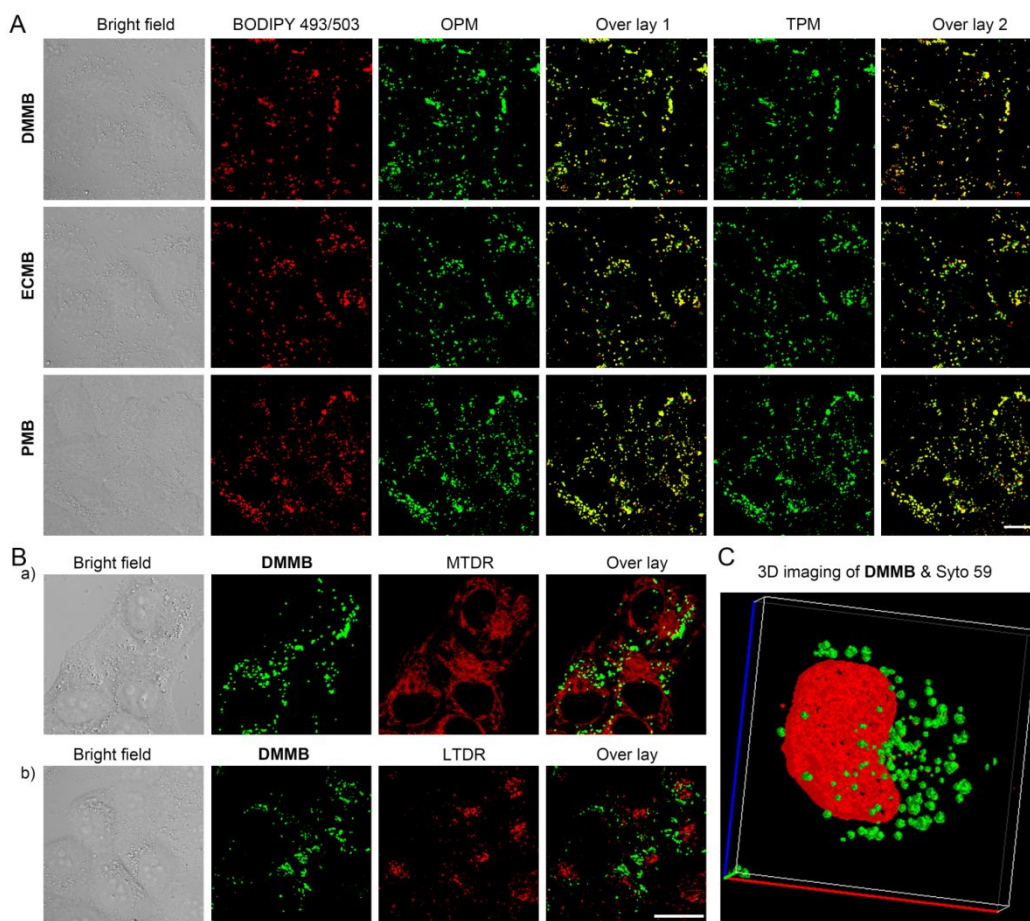


Figure 3. (A) The confocal images of the probes (20 μM) in living A549 cells co-stained with BODIPY 493/503 (1 $\mu\text{g}/\text{mL}$) for 30 min. $\lambda_{\text{ex}} = 405$ (OPM) and 850 nm (TPM) for the probes (green); $\lambda_{\text{ex}} = 488$ nm for BODIPY 493/503 (red). Overlay 1: Merged images of BODIPY493/503 signal and OPM signals of the probes. Overlay 2: Merged images of the BODIPY493/503 signal and TPM signals of the probes. Scale bar: 20 μm . (B) The LDs confocal images of **DMMB** (20 μM) with MTDR (a)/LTDR (b) ($\lambda_{\text{ex/em}} = 633/650 \pm 10$ nm) in living cells. Scale bar: 20 μm . (C) 3D images of A549 cells after incubation with **DMMB** (20 μM) and Syto 59 (100 ng/mL) for the LDs (green) and the nucleus (red).

Cell cytotoxicity assay and cell imaging. The cytotoxicity of the probes was firstly studied by standard MTT assay in A549 and HeLa cells according to a reported procedure.²⁶ As shown in Figure S5, the viability of cells was higher than 80% after incubation with 50 μM of probes for 24 h, demonstrating that the probes are biocompatible to living cells. BODIPY493/503 was performed to confirm the staining location of the probes. As shown in Figure 3A, the co-location images of the three probes for LDs present a point shape distribution in the cells, and the corresponding colocation coefficients of green-emissive the probes with BODIPY493/503 are calculated as 0.983 (**DMMB**), 0.832 (**ECMB**) and 0.887 (**PMB**), respectively, which indicates that the location of LDs with the probes is satisfactory. All of the

probes stained cells well with strong fluorescence at one-photon mode (OPM) and two-photon mode (TPM) (Figure 3A). Notably, **DMMB** presents a dotted shape distribution in cells and mainly accumulates on LDs. Compared with OPM, TPM has a better signal-to-noise ratio, which avoids the cell autofluorescence and background interference caused by short-wavelength excitation.¹⁶ The TPM co-localization data presented in Figure 3A further indicates that the probes could be enriched in LDs instead of the fluorescence of BODIPY 493/503 being re-excited. To detect the penetrating depth of **DMMB**, the analysis data of A549 cells treated with **DMMB** were recorded at both OPM and TPM. As shown in Figure S6, the A549 cells incubated with **DMMB** displays larger fluorescence emissive

penetration into the depth at TPM than that of OPM, illustrating that **DMMB** can track the spatial accumulation of LDs and their dynamic movement in living cells with good penetration by TPM.

To further investigate whether probe **DMMB** could target other organelles in cellular environment, we explored the co-location experiment of **DMMB** with three typical cellular markers: (i) MTDR for mitochondria, (ii) Lyso-Tracker Deep Red (LTDR) for Lysosome and (iii) Syto 59 for nucleic acid. As shown in Figure 3B and Figure S7, the dotted green fluorescence of **DMMB** barely merged with the red emission of MTDR, LTDR and Syto 59, suggesting **DMMB** was not targeted to mitochondria, lysosomes and nuclei. The photostability is a significant evaluation criterion for probes. Thus, the light bleaching properties of the probes together with commercially available LD-specific dye BODIPY493/503 were then investigated. As shown in Figure S8, it could be observed that the fluorescence of the cells stained with BODIPY493/503 is drastically lost, while the emissive signal of the aurone derivative probes is retained under the same conditions of 20 scans. The line series analysis for each group further verifies photostable character of the aurone probes (Figure S8D). The above research implies that the aurone probes have excellent photobleaching resistance and could be utilized for mapping LDs with good photostability in living cells. The 3D imaging of confocal microscope is usually obtained by Z-stack scanning, and therefore the sample need be scanned continuously for many times, which usually leads to the photobleaching of the fluorophore.⁴ Therefore, high quality 3D images can be obtained only when the probe has good fluorescence intensity and photostability. Here, **DMMB** allows excellent 3D imaging of LDs, which shows the cellular localization of LDs and the interrelations with nucleus more clearly (Figure 3C).

According to the reports from literatures,²⁸ oleic acid is taken up by cells and the phase splitting can occur, which results in a significant increase in the number of neutral lipids in cells, and cell fractionation shows that most newly synthesized neutrophils are concentrated in LDs together with LDs proteins. We treated the cells with nutrient rich substance of oleic acid. As shown in Figure 4A, an apparent green emission enhancement is observed after 6 h stimulation of oleic acid with the increasing concentration from 0 to 200 μM . The results reveal the accumulation of LDs and specific

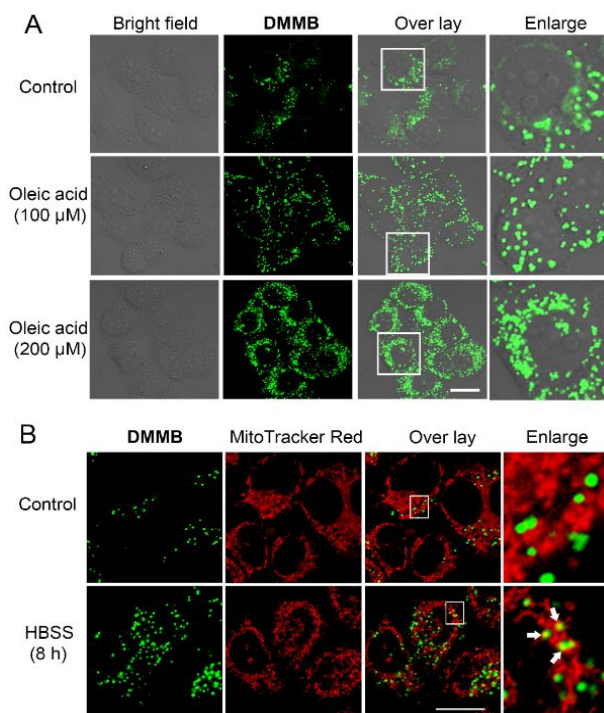


Figure 4. (A) Confocal images of A549 cells stained with **DMMB** (20 μM) after the cells were pre-treated with different concentrations of oleic acid (0, 100 and 200 μM) for 6 h. (B) Confocal images of A549 cells incubated in HBSS for 0 h (control) and 8 h, followed by staining with **DMMB** (20 μM , 30 min $\lambda_{\text{ex}} = 405$ nm) and Mito Tracker Red (100 nM, 30 min, $\lambda_{\text{ex}} = 543$ nm), respectively. Scale bar: 20 μm .

targeting ability of **DMMB** toward LDs in living cells. More meaningful, when living cells are in the early stage of starvation, they are under pressure to survive.^{29,30} The cells will activate related mechanisms (such as autophagy) to synthesize energy substances stored in LDs to meet the needs of future survival.^{15,31} Therefore, in the following experiments, the metabolism of LDs in the process of autophagy induced by cell starvation was carefully explored. After the cells were under the starvation of HBSS medium without serum for 8 h and then co-stained with **DMMB** and mito-tracker red for 30 min, two major phenomena were observed clearly (Figure 4B). First, the fluorescence of **DMMB** enhances obviously and increases intracellular distribution indicating the generation of LDs during nutrition stress for serum. Second, the mitochondria with red emission appears green colour from the **DMMB**-stained LDs compared with the control group, demonstrating the transportation of LDs from cytoplasm to mitochondria. The above interesting changes of LDs are

consistent with the recent study for the pathway of LDs catabolism, namely starvation-induced “lipophagy”.³²⁻³⁵ In the process of autophagic degradation of intracellular membranes, the formation of LDs in cells tends to transport the free fatty acids against its excessive accumulation and lipotoxicity.

LDs formation is a hallmark of cellular stress, but the LDs do not work in isolation.^{10,11} Cells always try to combat poisonous (such as, apoptosis and oxidative stress) stimuli by transforming their metabolism from oxidative phosphorylation to glycolysis.³⁶ ROS produced by H₂O₂ can induce apoptosis and decrease mitochondrial membrane potential (MMP).^{12,13,18} Large excess of H₂O₂ can directly stimulate cells to produce oxidative stress response in a short time, resulting in MMP collapse or even damage.^{20,21} Mitochondria-LDs contactation promotes the transfer of FAs for β -oxidation in mitochondria.¹⁵ But in this process, the dynamic change between LDs and mitochondria is still unclear. Commercial mitochondrial dyes MTR and MTDR are commonly used to track changes in MMP in cells.³⁷⁻³⁹ During apoptosis, mitochondrial dysfunction can also cause extensive LDs formation.⁶ Currently, MTR and LDs dyes have been used to track the fusion process of mitochondria and LDs during H₂O₂ inducing apoptosis in real time.¹⁸ However, to the best of our knowledge, the real-time tracking dynamic changes between LDs and mitochondria when the cells are under oxidative stress have not been reported.

As shown in Figure 5A, H₂O₂ (10 mM) was added to A549 cells pretreated with MTDR and **DMMB** and the cells were further incubated for 20 minutes. As time goes on, the fluorescence of LDs stained with **DMMB** remains stable, and the red fluorescence of mitochondria gradually diffuses and disappears after 20 minutes. At the same time, in the overlay layer, it can be clearly seen that the green and red fluorescence gradually merge on the LDs (yellow spots). It is worth noting that the position of the LDs does not shift significantly during the entire process. Interestingly, this phenomenon is significantly different from the LDs and mitochondrial fusion observed in the case of ROS inducing apoptosis, in which, mitochondrial morphology changes and LDs move around the mitochondria to undergo autophagy.^{18,36,40,41} The main reason may be that MMP collapses and mitochondria damages due to the oxidative stress response of cells stimulated by high concentrations of H₂O₂.^{20,21} The chloromethyl-containing MTDR reacts with the thiol groups of mitochondrial proteins

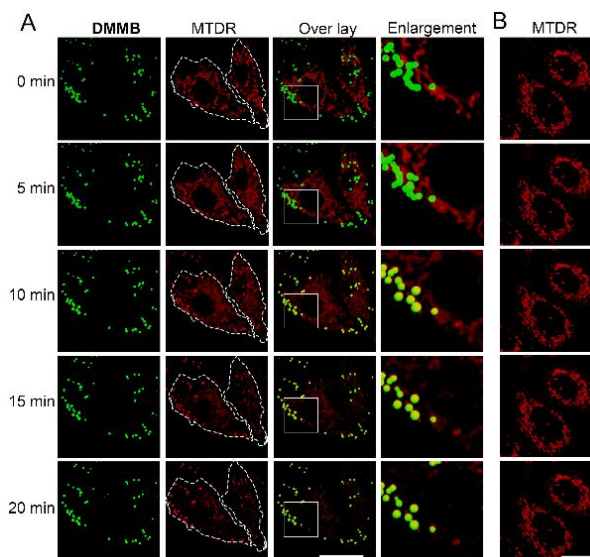


Figure 5. (A) The confocal images of **DMMB** and **MTDR**-stained A549 cells treated with 10 mM H₂O₂. (B) Control experiment, **MTDR**-stained A549 cells were scanned continuously under the same laser intensity. Scale bar: 20 μ m.

to form lipid-soluble conjugates, which escapes from mitochondria due to mitochondrial damage and the decrease in MMP, those lipid-soluble conjugates then enter **DMMB**-stained LDs.^{20,42} Considering that **MTDR** may be bleached, comparative experiments were presented. As shown in Figure 5B, the red fluorescence of A549 cells only staining with **MTDR** does not change significantly under the same conditions. Under oxidative stress, mitochondria collapse and the lipid-soluble conjugates are fused by LDs, suggesting that LDs play a protective antioxidant role in cells.^{43,44} At subcellular organelle level, the direct impact of oxidative stress on mitochondrial-lipid interactions was enriched the content of the mitochondrial-lipid interaction network. We have also studied the polarity changes of LDs of A549 cells in a large amount of H₂O₂ in a short period of time.²⁰ As shown in Figure S9, the colour changes of the fluorescence in green and red channels are similar to the red shift of **DMMB** caused by the increase of the solvent polarity, which indicates that the polarity of LDs in A549 cells increases significantly at this case. LDs are closely connected with many physiological processes and abnormal LDs are related to many diseases including hepatocellular carcinoma, atherosclerosis and cancer. Research on the effect of oxidative stress in LDs may open up a new avenue for exploring their biological metabolism devoting to the early diagnosis of related diseases.

CONCLUSIONS

In summary, three aurone derivatives as LDs markers have been successfully developed. The cell imaging experiments demonstrate that all of them could specifically stain LDs with striking photostability. Additionally, one of the aurone derivatives, **DMMB** provides a direct way to visualize the metabolism of LDs under either nutrient-rich oleic acid or starvation stress of serum indicating the formation and transporting function in autophagy period of LDs. **DMMB** also can be used to trace membrane integrity of mitochondria during the oxidative stress. Notably, the dynamic change between mitochondria and LDs when mitochondrial damage is caused by a large excess of H₂O₂ in a short time was observed for the first time by using **DMMB**. Thus, based on the aurone derivative solvatochromic dye, we propose a concept of Mitochondria-LDs interaction network for monitoring their response to metabolism and oxidative stress, which may be useful for the early diagnosis of related diseases.

ASSOCIATED CONTENT

Supporting Information

The Supporting Information is available free of charge on the ACS Publications website at DOI:

Experimental details, additional UV-vis absorption, fluorescence data and imaging.

AUTHOR INFORMATION

Corresponding Author

* E-mail: duxiaocao@ujn.edu.cn.

* E-mail: weivinglin2013@163.com.

ORCID

Kangnan Wang: 0000-0002-0835-8803

Yanyan Ma: 0000-0002-9358-5866

Duxia Cao: 0000-0002-9452-4045

Weiyang Lin: 0000-0001-8080-4102

Notes

The authors declare no competing financial interest.

ACKNOWLEDGEMENTS

This work was supported by the National Natural Science Foundation of China (21472067, 21672083, 21877048, 21672130), the Natural Science Foundation of Shandong Province (ZR2017MEM006), Taishan Scholar Foundation (TS201511041), the startup fund of University of Jinan (309-10004), and China Postdoctoral Science Foundation (2019M662968).

REFERENCES

- (1) Beller, M.; Thiel, K.; Thul, P. J.; Jäckle, H. Lipid Droplets: A Dynamic Organelle Moves Into Focus. *FEBS Lett.* **2010**, *584*, 2176-2182.
- (2) Fam, T. K.; Klymchenko, A. S.; Collot, M. Recent Advances in Fluorescent Probes for Lipid Droplets. *Materials* **2018**, *11*, 1768.
- (3) Fujimoto, T.; Parton, R. G. Not Just Fat: The Structure and Function of the Lipid Droplet. *Cold Spring Harb Perspect Biol.* **2011**, *3*, a004838.
- (4) Collot, M.; Fam, T. K.; Ashokkumar, P.; Faklaris, O.; Galli, T.; Danglot, L.; Klymchenko, A. S. Ultrabright and Fluorogenic Probes for Multicolor Imaging and Tracking of Lipid Droplets in Cells and Tissues. *J. Am. Chem. Soc.* **2018**, *140*, 5401-5411.
- (5) Yu, L.; Chen, Y.; Tooze, S. A. Autophagy Pathway: Cellular and Molecular Mechanisms. *Autophagy* **2018**, *14*, 207-215.
- (6) Boren, J.; Brindle, K. M. Apoptosis-Induced Mitochondrial Dysfunction Causes Cytoplasmic Lipid Droplet Formation. *Cell Death Differ.* **2012**, *19*, 1561-1570.
- (7) Cohen, J. C.; Horton, J. D.; Hobbs, H. H. Human Fatty Liver Disease: Old Questions and New Insights. *Science* **2011**, *332*, 1519-1523.
- (8) Krahrmer, N.; Farese, R. V.; Walther, T. C. Balancing the Fat: Lipid Droplets and Human Disease. *EMBO Mol. Med.* **2013**, *5*, 973-983.
- (9) Liu, Q.; Luo, Q.; Halim, A.; Song, G. Targeting Lipid Metabolism of Cancer Cells: A Promising Therapeutic Strategy for Cancer. *Cancer Lett.* **2017**, *401*, 39-45.
- (10) Boroughs, L. K.; DeBerardinis, R. J. Metabolic Pathways Promoting Cancer Cell Survival and Growth. *Nat. Cell Biol.* **2015**, *17*, 351-359.
- (11) Jeon, S. M.; Chandel, N. S.; Hay, N. AMPK Regulates NADPH Homeostasis to Promote Tumour Cell Survival During Energy Stress. *Nature* **2012**, *485*, 661-665.
- (12) Yee, C.; Yang, W.; Hekimi, S. The Intrinsic Apoptosis Pathway Mediates the Pro-Longevity Response to Mitochondrial ROS in *C. elegans*. *Cell* **2014**, *157*, 897-909.
- (13) Tang, X. Q.; Feng, J. Q.; Chen, J.; Chen, P. X.; Zhi, J. L.; Cui, Y.; Guo, R. X.; Yu, H. M. Protection of Oxidative Preconditioning Against Apoptosis Induced by H₂O₂ in PC12 cells: Mechanisms via MMP, ROS, and Bcl-2. *Brain Res.* **2005**, *1057*, 57-64.
- (14) Liu, L.; Zhang, K.; Sandoval, H.; Yamamoto, S.; Jaiswal, M.; Sanz, E.; Li, Z.; Hui, J.; Graham, B. H.; Quintana, A.; Bellen, H. J. Glial Lipid Droplets and ROS Induced by Mitochondrial Defects Promote Neurodegeneration. *Cell* **2015**, *160*, 177-190.

- (15) Henne, W. M.; Reese, M. L.; Goodman, J. M. The Assembly of Lipid Droplets and Their Roles in Challenged Cells. *EMBO J.* **2018**, *37*, e98947.
- (16) Yin, J.; Peng, M.; Lin, W. Two-Photon Fluorescence Imaging of Lipid Droplets Polarity Toward Cancer Diagnosis in Living Cells and Tissue. *Sens. Actuators, B: Chem.* **2019**, *288*, 251-258.
- (17) Jiang, N.; Fan, J.; Xu, F.; Peng, X.; Mu, H.; Wang, J.; Xiong, X. Ratiometric Fluorescence Imaging of Cellular Polarity: Decrease in Mitochondrial Polarity in Cancer Cells. *Angew. Chem. Int. Ed.* **2015**, *54*, 2510-2514.
- (18) Dang, D.; Liu, H.; Wang, J.; Chen, M.; Liu, Y.; Sung, H. H. Y.; Williams, I. D.; Kwok, R. T. K.; Lam, J. W. Y.; Tang, B. Z. Highly Emissive AIEgens with Multiple Functions: Facile Synthesis, Chromism, Specific Lipid Droplet Imaging, Apoptosis Monitoring, and In Vivo Imaging. *Chem. Mater.* **2018**, *30*, 7892-7901.
- (19) Ashoka, A. H.; Ashokkumar, P.; Kovtun, Y. P.; Klymchenko, A. S. Solvatochromic Near-Infrared Probe for Polarity Mapping of Biomembranes and Lipid Droplets in Cells under Stress. *J. Phys. Chem. Lett.* **2019**, *10*, 2414-2421.
- (20) Wu, S.; Zhou, F.; Zhang, Z.; Xing, D. Mitochondrial Oxidative Stress Causes Mitochondrial Fragmentation via Differential Modulation of Mitochondrial Fission-Fusion Proteins. *FEBS J.* **2011**, *278*, 941-954.
- (21) Kowluru, R. A.; Mishra, M. Oxidative Stress, Mitochondrial Damage and Diabetic Retinopathy. *Biochim. Biophys. Acta* **2015**, *1852*, 2474-2483.
- (22) Listenberger, L. L.; Brown, D. A. Fluorescent Detection of Lipid Droplets and Associated Proteins. *Curr. Protoc. Cell Biol.* **2007**, *35*, 24.
- (23) Velikkakath, A. K.; Nishimura, T.; Oita, E.; Ishihara, N.; Mizushima, N. Mammalian Atg2 Proteins are Essential for Autophagosome Formation and Important for Regulation of Size and Distribution of Lipid Droplets. *Mol. Biol. Cell.* **2012**, *23*, 896-909.
- (24) Rambold, A. S.; Cohen, S.; Lippincott-Schwartz, J. Fatty Acid Trafficking in Starved Cells: Regulation by Lipid Droplet Lipolysis, Autophagy, and Mitochondrial Fusion Dynamics. *Dev. Cell* **2015**, *32*, 678-92.
- (25) Ma, L.; Sun, Y.; Cao, D.; Chen, H.; Liu, Z.; Fang, Q. Synthesis, Crystal Structure and Two-Photon Excited Fluorescence Properties of Three Aurone Derivatives. *Spectrochim. Acta A* **2013**, *103*, 120-124.
- (26) Wang, K. N.; Cao, Q.; Liu, L. Y.; Zhao, Z. J.; Liu, W.; Zhou, D. J.; Tan, C. P.; Xia, W.; Ji, L. N.; Mao, Z. W. Charge-Driven Tripod Somersault on DNA for Ratiometric Fluorescence Imaging of Small Molecules in The Nucleus. *Chem. Sci.* **2019**, *10*, 10053-10064.
- (27) Singh, M. K.; Shweta, H.; Khan, M. F.; Sen, S., New Insight Into Probe-Location Dependent Polarity and Hydration at Lipid/water Interfaces: Comparison Between Gel- and Fluid-phases of Lipid Bilayers. *Phys. Chem. Chem. Phys.* **2016**, *18*, 24185-24197.
- (28) Fujimoto, Y.; Onoduka, J.; Homma, K. J.; Yamaguchi, S.; Mori, M.; Higashi, Y.; Makita, M.; Kinoshita, T.; Noda, J.; Itabe, H.; Takano, T. Long-Chain Fatty Acids Induce Lipid Droplet Formation in a Cultured Human Hepatocyte in a Manner Dependent of Acyl-CoA Synthetase. *Biol. Pharm. Bull.* **2006**, *29*, 2174-2780.
- (29) Rambold, A. S.; Cohen, S.; Lippincott-Schwartz, J. Fatty Acid Trafficking in Starved Cells: Regulation by Lipid Droplet Lipolysis, Autophagy, and Mitochondrial Fusion Dynamics. *Dev. Cell.* **2015**, *32*, 678-692.
- (30) Velázquez, A. P.; Tatsuta, T.; Ghillebert, R.; Drescher, I.; Graef, M. Lipid Droplet-Mediated ER Homeostasis Regulates Autophagy and Cell Survival During Starvation. *J. Cell Biol.* **2016**, *212*, 621-631.
- (31) Filomeni, G.; Zio, D. D.; Cecconi, F. Oxidative Stress and Autophagy: the Clash Between Damage and Metabolic Needs. *Cell Death Differ.* **2015**, *22*, 377-388.
- (32) Nguyen, T. B.; Louie, S. M.; Daniele, J. R.; Tran, Q.; Dillin, A.; Zoncu, R.; Nomura, D. K.; Olzmann, J. A. DGAT1-Dependent Lipid Droplet Biogenesis Protects Mitochondrial Function During Starvation-Induced Autophagy. *Dev. Cell.* **2017**, *42*, 9-21.
- (33) Nguyen, T. B.; Olzmann, J. A. Lipid Droplets and Lipotoxicity During Autophagy. *Autophagy* **2017**, *13*, 2002-2003.
- (34) Barbosa, A. D.; Siniosoglou, S. Spatial Distribution of Lipid Droplets During Starvation: Implications for Lipophagy. *Commun. Integr. Biol.* **2016**, *9*, e1183854.
- (35) Liu, K.; Czaja, M. J. Regulation of Lipid Stores and Metabolism by Lipophagy. *Cell Death Differ.* **2013**, *20*, 3-11.
- (36) Lee, S. J.; Zhang, J.; Choi, A. M. K.; Kim, H. P. Mitochondrial Dysfunction Induces Formation of Lipid Droplets as a Generalized Response to Stress. *Oxid. Med. Cell. Longevity* **2013**, *2013*, 327167.
- (37) Gilmore, K.; Wilson, M. The Use of Chloromethyl-X-Rosamine (Mitotracker Red) to Measure Loss of Mitochondrial Membrane Potential in Apoptosis Cells Is Incompatible with Cell Fixation. *Cytometry* **1999**, *36*, 355-358.

- (38) Lugli, E.; Troiano, L.; Ferraresi, R.; Roat, E.; Prada, N.; Nasi, M.; Pinti, M.; Cooper, E. L.; Cossarizza, A. Characterization of cells with different mitochondrial membrane potential during apoptosis. *Cytometry A* **2005**, *68*, 28-35.
- (39) Smaili, S. S.; Hsu, Y. T.; Sanders, K. M.; Russell, J. T.; Youle, R. J. Bax Translocation to Mitochondria Subsequent to a Rapid Loss of Mitochondrial Membrane Potential. *Cell Death Differ.* **2001**, *8*, 909-920.
- (40) Simon, H.; Haj-Yehia, A.; Levi-Schaffer, F. Role of Reactive Oxygen Species (ROS) in Apoptosis Induction. *Apoptosis* **2000**, *5*, 415-418.
- (41) Ly, J. D.; Grubb, D. R.; Lawen, A. The Mitochondrial Membrane Potential ($\Delta\Psi_m$) in Apoptosis; an Update. *Apoptosis* **2003**, *8*, 115-128.
- (42) Poot, M.; Zhang, Y. Z.; Krämer, J. A.; Wells, K. S.; Jones, L. J.; Hanzel, D. K.; Lugade, A. G.; Singer, V. L.; Haugland, R. P. Analysis of Mitochondrial Morphology and Function with Novel Fixable Fluorescent Stains. *J. Histochem. Cytochem.* **1996**, *44*, 1363-1372.
- (43) Jarc, E.; Kump, A.; Malavasic, P.; Eichmann, T. O.; Zimmermann, R.; Petan, T., Lipid Droplets Induced by Secreted Phospholipase A2 and Unsaturated Fatty acids Protect Breast Cancer Cells from Nutrient and Lipotoxic Stress. *Biochim. Biophys. Acta. Mol. Cell. Biol. Lipids.* **2018**, *1863*, 247-265.
- (44) Bailey, A. P.; Koster, G.; Guillemier, C.; Hirst, E. M.; MacRae, J. I.; Lechene, C. P.; Postle, A. D.; Gould, A. P., Antioxidant Role for Lipid Droplets in a Stem Cell Niche of *Drosophila*. *Cell* **2015**, *163*, 340-353.

A Table of contents (TOC) graphic

